

Enteroendocrine cells sense bacterial tryptophan catabolites to activate enteric and vagal neuronal pathways

Lihua Ye, Munhyung Bae, Chelsi D. Cassilly, Sairam V. Jabba, Daniel W. Thorpe, Alyce M Martin, Hsiu-Yi Lu, Jinhu Wang, John D. Thompson, Colin R. Lickwar, Kenneth D. Poss, Damien J. Keating, Sven-Eric Jordt, Jon Clardy, Rodger A. Liddle, and John F. Rawls

SUPPLEMENTAL FIGURES

Figure S1. *E. tarda* activates EECs *in vivo*, related to Main Figure 1. (A) Epifluorescence image of *Tg(neurod1:CaMPARI)* zebrafish without UV conversion. Note that there is no red CaMPARI signal (magenta) in A'. (B) Confocal image of intestinal EECs in *Tg(neurod1:CaMPARI)* zebrafish without UV conversion. (C) Epifluorescence image of unstimulated *Tg(neurod1:CaMPARI)* zebrafish post UV conversion. The red CaMPARI signal is apparent in CNS and islets in C'. (D-F') Confocal image of intestinal EECs (D, D'), CNS (E, E') and islets (F, F') in unstimulated *Tg(neurod1:CaMPARI)* zebrafish after UV conversion. (G) Schematic of liver, pancreas and intestine in 6 dpf zebrafish larvae. The intestinal region that is imaged to assess the CaMPARI signal is indicated by a red box. (H-J) Quantification of EEC red:green CaMPARI fluorescence ratio in water- and linoleate-stimulated zebrafish. (K) Schematic of *in vivo* EEC Gcamp recording in response to bacterial stimulation in *Tg(neurod1:Gcamp6f)* zebrafish. (L) Quantification of EEC Gcamp6f fluorescence in response to stimulation by different bacteria. (M) Quantification of EEC Gcamp6f fluorescence before and 20 mins after *E. tarda* administration. (N-O) Fluorescence image of zebrafish intestine in *Tg(neurod1:Gcamp6f)* zebrafish without treatment (N) or 5 hours post *E. tarda* treatment (O). (P) Quantification of EEC Gcamp6f fluorescence in zebrafish without or with *E. tarda* treatment. Student's t-test was used in M and P for statistical analysis. * $p < 0.05$.

Figure S2. EECs express *trpa1b* and respond to Trpa1 agonist, related to Main Figure 2 and Figure 3. (A) Normalized counts of *trpa1a* and *trpa1b* gene expression in zebrafish EECs and other IECs from zebrafish EEC RNA-seq data (Table S1). (B) Gel image of PCR product from FACS sorted EECs and other IECs cell population using primers from *trpa1a*, *trpa1b* and *18S*. (C) Epifluorescence image of *trpa1b*^{+/+} (left) and *trpa1b*^{-/-} (right) *Tg(neurod1:Gcamp6f)* zebrafish before or 2 mins post Trpa1 agonist AITC stimulation. (D) Epifluorescence image of *Tg(neurod1:Gcamp6f)* zebrafish following AITC stimulation with or without Trpa1 antagonist HC030031 treatment. (E) Epifluorescence image of *trpa1a*^{+/+} and *trpa1a*^{-/-} *Tg(neurod1:Gcamp6f)* zebrafish 2 mins after AITC stimulation. (F) Quantification of EEC Gcamp fluorescence signal in *trpa1a*^{+/+}, *trpa1a*^{+/-} and *trpa1a*^{-/-} zebrafish. (G) Confocal projection of *trpa1b*^{+/+} and *trpa1b*^{-/-} *Tg(neurod1:CaMPARI)* zebrafish after AITC stimulation and UV light photoconversion. (H) Model of gut bacterial CFU quantification. (I) Quantification of gut bacterial CFU in *trpa1b*^{+/+}, *trpa1b*^{+/-} and *trpa1b*^{-/-} conventionalized zebrafish. (J) Epifluorescence image of WT, *Tg(neurod1:cre)*, *Tg(gata5:RSD)* and *Tg(neurod1:cre); Tg(gata5:RSD)* zebrafish. The EECs in all the groups are labelled by *Tg(neurod1:EGFP)*. Note that *neurod1:EGFP* labelling is largely absent in *Tg(neurod1:cre); Tg(gata5:RSD)* zebrafish indicating EEC ablation. (K) Confocal images of *Tg(neurod1:cre)* (left) and *Tg(neurod1:cre); Tg(gata5:RSD)* (right) zebrafish intestine stained with PYY antibody. Yellow arrows in D indicate PYY⁺ EECs. (L) qPCR analysis of EEC marker genes, other IEC marker genes and neuronal genes in WT and EEC-ablated zebrafish. (M) Quantification of zebrafish survival rate when treated with different doses of *E. tarda* FL6-60. (N) Representative

image of zebrafish treated with 10^6 CFU/ml or 10^7 CFU/ml *E. tarda*. Note that in the 10^6 CFU/ml treated zebrafish, the majority of the surviving zebrafish do not exhibit gross pathology (top image). While many of the surviving zebrafish treated with 10^7 CFU/ml *E. tarda* displayed deflated swim bladder, altered intestinal morphology and ruptured skin (bottom image). (O) Quantification of gut bacterial CFU in WT, *Tg(neurod1:cre)*, *Tg(gata5:RSD)* and *Tg(neurod1:cre); Tg(gata5:RSD)* conventionalized zebrafish. (P) Epifluorescence image of *Tg(gata5:RSD)* and EEC-ablated zebrafish treated with *E. tarda* mCherry for 3 days. (Q) Quantification of *E. tarda* mCherry fluorescence intensity in the intestinal lumen of *Tg(gata5:RSD)* or EEC-ablated zebrafish. One-way ANOVA with Tukey's post test was used in F, I, L, O and student t-test was used in Q for statistical analysis. n.s. (not significant), * $p < 0.05$, ** $p < 0.01$, *** $p < 0.001$.

Figure S3. Activation of EEC Trpa1 signaling promotes intestinal motility, related to Main Figure 4. (A) Experimental design for activating EEC Trpa1 signaling using Optovin-UV. (B) Confocal image of *Tg(neurod1:Gcamp6f); Tg(neurod1:TagRFP)* zebrafish intestine before (images on the left) and after (images on the right) UV light activation. Yellow arrows indicate the subpopulation of EECs exhibiting increased Gcamp fluorescence following UV activation. (C) Quantification of the EEC Gcamp6f to TagRFP fluorescence ratio before and after UV activation. (D) Schematic of intestinal movement in larval zebrafish. The proximal zebrafish intestine exhibits retrograde movement while mid-intestine and distal intestine exhibit anterograde movement. The imaged and UV light activated intestinal region in the Optovin-UV experiment is indicated by the red box. The μ velocity indicates intestinal horizontal movement. A positive value indicates anterograde movement and a negative value indicates retrograde movement. The v velocity indicates intestinal vertical movement. (E) Quantification of intestinal motility using PIV-LAB velocity analysis before and after UV activation. Note that Optovin-UV induced Trpa1 activation increased μ velocity (horizontal movement) more than v velocity (vertical movement). (F) Confocal image of ChR2+Trpa1+ EECs (yellow circles, top image) and ChR2+Trpa1- EECs (red circles, bottom image) in *TgBAC(trpa1b:EGFP); Tg(neurod1:Gal4); Tg(UAS:ChR2-mCherry)* zebrafish. (G) Quantification of μ velocity following blue light activation of ChR2+Trpa1+ or ChR2+Trpa1- EECs. (H) Quantification of mean intestinal velocity magnitude change before and after blue light activation of ChR2+Trpa1- EECs. (I) Quantification of mean intestinal velocity magnitude in response to *E. tarda* gavage in *trpa1b+/+* or *trpa1b-/-* zebrafish. Student t-Test was used in I. *** $P < 0.001$.

Figure S4. The role of the enteric nervous system in EEC Trpa1-induced intestinal motility, related to Main Figure 5. (A-B) Epifluorescence image of *ret+/+* or *ret+/-* (*ret+/?*, A) and *ret-/-* (B) *Tg(NBT:DsRed); Tg(neurod1:EGFP)* zebrafish. The intestines are denoted by white dash lines. (C-D) Epifluorescence image of *ret+/? Tg(neurod1:Gcamp6f)* zebrafish before (C) and 2 mins after AITC stimulation (D). (E-F) Epifluorescence image of *ret-/- Tg(neurod1:Gcamp6f)* zebrafish before (E) and 2 mins after AITC stimulation (F). (G) Quantification of *ret+/?* and *ret-/-* intestinal μ velocity following Optovin-UV-induced Trpa1 activation. (H) Quantification of velocity before and after Optovin-UV-induced Trpa1 activation in *ret+/?* and *ret-/-* zebrafish. (I-J) Confocal projection of *sox10+/?* zebrafish intestine stained with Zn12 (I, magenta, ENS labeling) or 2F11 (J, green, EEC labeling). (K-L) Confocal projection of *sox10-/-* zebrafish intestine stained with zn-12 (K) or 2F11 (L). (M-N) Quantification of changes in mean intestinal velocity magnitude before and after Optovin-UV activation in *sox10+/?* (M) or *sox10-/-* (N) zebrafish. (O-P) Confocal projection of *TgBAC(trpa1b:EGFP)* zebrafish intestine stained with Desmin (myoblast or smooth muscle cell marker, O') or Zn12 (ENS marker, P'). (Q) Confocal image of *TgBAC(trpa1b:EGFP); Tg(NBT:DsRed)* zebrafish intestine. Note in P and Q that both Zn12+ ENS and NBT+ ENS are

trpa1b⁻. (R) Confocal image of *TgBAC(chata:Gal4); Tg(UAS:NTR-mCherry); TgBAC(trpa1b:EGFP)* zebrafish intestine. Note that the *chata*⁺ ENS are *trpa1b*⁻.

Figure S5. Zebrafish EECs directly communicate with *chata*⁺ ENS, related to Main Figure 5. (A-B) Confocal projection of 6 dpf (A) and adult (B) *Tg(neurod1:EGFP)* zebrafish intestine stained with the neuronal marker synaptic vesical protein 2 (SV2, magenta) antibody. (C) Higher magnification view of an EEC that exhibiting a neuropod contacting SV2 labelled neurons in the intestine. Yellow arrow indicates the EEC neuropod is enriched in SV2. (D) Higher magnification view of an EEC and neuropod in *Tg(neurod1:TagRFP); Tg(neurod1:mitoEOS)* zebrafish. The yellow arrow indicates the EEC neuropod is enriched in mitochondria (green, labelled by *neurod1:mitoEOS*). (E) Confocal projection of *chata*⁺ ENS in *TgBAC(chata:Gal4); Tg(UAS:mCherry-NTR)* zebrafish intestine. Asterisks indicate the *chata*⁺ enteric neuron cell bodies. (F) Higher magnification view of a *chata*⁺ ENS (white arrow in E). The nuclei of this *chata*⁺ enteric neuron is shown on the right. (F') The axon processes of the *chata*⁺ enteric neuron. Note this neuron displays a typical Dogiel type II morphology in which multiple axons project from the cell body. (G) Confocal projection of *chata*⁺ ENS and EECs in *TgBAC(chata:Gal4); Tg(UAS:mCherry-NTR); Tg(neurod1:EGFP)* zebrafish intestine. EECs are labeled as green and *chata*⁺ ENS are labeled as magenta. Asterisks indicate the *chata*⁺ enteric neuron cell bodies. (H) Higher magnification view of the physical connection between EECs and the *chata*⁺ enteric neuron. Yellow arrow indicates an EEC forming a neuropod to contact a *chata*⁺ enteric neuron. (I) Confocal projection of EECs (2F11⁺, green) and *chata*⁺ ENS (magenta) in *TgBAC(chata:Gal4); Tg(UAS: NTR-mCherry)* zebrafish. An asterisk indicates the *chata*⁺ ENS cell body. (J) Higher magnification view of the connection between EECs and *chata*⁺ ENS fibers. The point where EECs connected with *chata*⁺ nerve fibers are indicated by yellow arrows. (K) Schematic of Optovin-UV experiment in zebrafish that are anatomically disconnected from their CNS. The Optovin-treated zebrafish were mounted and placed on a confocal objective station. Immediately prior to imaging, the head of the mounted zebrafish was quickly removed with a sharp razor blade and imaging was then performed. (L) Quantification of the mean intestinal velocity before and post UV treatment in decapitated zebrafish. (M) Schematic and confocal image shows the *chata*⁺ ENS which is labelled by both *Gcamp6s* and *mCherry* in decapitated *TgBAC(chata:Gcamp6s); Tg(UAS:Gcamp6s); Tg(UAS:NTR-mCherry)* zebrafish. (N) Confocal image shows the *chata*⁺ ENS *Gcamp* fluorescence intensity before and post *Trpa1*⁺ EEC activation by UV light. (O) Quantification of relative *chata*⁺ ENS *Gcamp* fluorescence intensity before and post *Trpa1*⁺ EEC activation. The *Gcamp* fluorescence intensity was normalized to *mCherry* fluorescence. n=12 from 7 zebrafish. (P) Log₂ fold change of presynaptic genes in zebrafish, mouse and human EECs (Table S2). (Q-R) Confocal image and higher magnification view of *TgBAC(trpa1b:EGFP); Tg(tph1b:mCherry-NTR)* zebrafish intestine showing the *tph1b*⁺ (magenta) *trpa1b*⁺ (green). (S) Quantification of *tph1a* and *tph1b* in zebrafish EECs. (T) Quantification of 5-HT⁺ or *tph1b*⁺ EECs. (U) Quantification of *tph1b*⁺ and *trpa1b*⁺ EECs. Note the majority of *tph1b*⁺ EECs are *trpa1b*⁺. (V) Quantification of mean intestinal μ velocity in unstimulated *tph1b*^{+/-} and *tph1b*^{-/-} zebrafish. Student t-test was used in V.

Figure S6. Zebrafish vagal sensory nerve innervate the intestine, related to Main Figure 6. (A-B) Lightsheet imaging of the right (A) and left (B) side of zebrafish intestine stained with acetylated α -tubulin antibody (white). (C) Schematic diagram of the Vagal-Brainbow model to label vagal sensory cells using *Tg(neurod1:cre); Tg(β act2:Brainbow)* zebrafish. See Vagal-Brainbow projection in Fig. 6F. (D) Confocal image of vagal ganglia in brainbow zebrafish stained with GFP antibody (green). Note that GFP antibody recognizes both YFP⁺ and CFP⁺ vagal

sensory neurons. Six branches (V_i to V_{vi}) extend from the vagal sensory ganglia and branch V_{vi} innervates the intestine. (E-E') Confocal image of vagal sensory ganglia in brainbow zebrafish showing that V_{vi} exits from the ganglia and courses behind the esophagus. (F-G) Confocal image of the proximal (F) and distal (G) intestine in brainbow zebrafish. The vagus nerve (green) innervates both intestinal regions. (H) Confocal image of vagal sensory ganglia in *Tg(isl1:EGFP); Tg(neurod1:TagRFP)* zebrafish. The vagal sensory ganglia is indicated by a yellow circle. The asterisk indicates the posterior lateral line ganglion. Note that *isl1* (green) is expressed in the vagal sensory ganglia and overlaps with *neurod1* (magenta). (I) Confocal image of intestine in *Tg(isl1:EGFP); Tg(neurod1:TagRFP)* zebrafish. The vagus nerve is labelled by *isl1* (green) and the intestinal EECs are labelled by *neurod1* (magenta). (J) Confocal plane of intestine in *Tg(isl1:EGFP); Tg(neurod1:TagRFP)* zebrafish. Note that the V_{vi} branch of the vagus nerve is labelled by *isl1* and travels behind the esophagus to innervate the intestine. (K) Schematic of *in vivo* vagal calcium imaging in PBS or AITC gavaged zebrafish. (L) *In vivo* vagal calcium imaging of *Tg(neurod1:TagRFP); Tg(neurod1:Gcamp6f)* zebrafish without gavage, gavaged with PBS or gavaged with AITC.

Figure S7. *E. tarda* secretes tryptophan catabolites indole and IAld that activate Trpa1, related to Main Figure 7. (A) Chemical profiles of Trp-Indole derivatives from supernatants of *E. tarda* in nutrient-rich TSB media. (B) Screening of supernatants of *E. tarda* in TSB media. Samples for *E. tarda* in TSB culture were collected at 0, 6, 18, and 24 h. (C) Screening of supernatants of *E. tarda* in TSB media. Abbreviations are as follows: IAld, indole-3-carboxaldehyde; IET, tryptophol; IAM, indole-3-acetamide; IAA, indole-3-acetic acid; IAAlD, indole-3-acetaldehyde; and IpyA, indole-3-pyruvate. Extracted ions were selected for IAld (m/z 145), IET, (m/z 161), Indole (m/z 117), IAAlD (m/z 159), IAM (m/z 174), IAA (m/z 175), and IpyA (m/z 203). (D) Chemical profiles of Trp-Indole derivatives from supernatants of various commensal bacteria in TSB medium for 1 day of cultivation. Y-axis values represent production of Trp-Indole derivatives normalized to CFU, with each strain beginning at zero. (E) Proposed model of *E. tarda* tryptophan catabolism. (F) EEC Gcamp fluorescence intensity in *Tg(neurod1:Gcamp6f)* zebrafish stimulated with different tryptophan catabolites. (G-H) Represented images (G) and quantification (H) of activated EECs in *Tg(neurod1:CaMPARI)* zebrafish that is stimulated with PBS or with CFS from *E. tarda* 23685 and *E. tarda* 15974. (I-J) Indole (I) and IAld (J) stimulation of Ca^{2+} influx in human TRPA1 expressing HEK-293T cells, measured as fluorescence increase of intracellular Calcium 6 indicator. (K-L) Effects of TRPA1 inhibition using various concentrations of inhibitor A967079, on subsequent Ca^{2+} influx in response to indole (100 μ M, G) or, IAld (100 μ M, H) in human TRPA1 expressing HEK-293T cells. Data are from a representative experiment performed in triplicate and repeated three times. (M-N) Sensitivity of mouse TRPA1 to indole and IAld. (M) Dose-response effects of indole and IAld (EC50 = 130.7 μ M, 107.8 – 158.4 μ M 95% CI for Indole; and, EC50 = 189.0 μ M, 132.8 - 268.8 μ M 95% CI for IAld). Concentration-response data were normalized to 1 mM cinnamaldehyde (CAD), a known TRPA1 agonist. (N) Effects of the Trpa1 inhibitor A967079, on $[Ca^{2+}]_i$ in response to 100 μ M indole in mouse Trpa1-expressing HEK-293T cells. Cells were treated with A967079 before the addition of indole (100 μ M). Changes in Calcium 6 fluorescence above baseline (Fmax-F0; maximal $[Ca^{2+}]_i$) are expressed as a function of Trpa1 inhibitor, A967079, concentration (IC50 = 315.5 nM, 202.3 – 702.3 nM 95% CI for indole). Concentration-response data were normalized to the response elicited by 100 μ M Indole. Data represent mean \pm s.e.m. of normalized measures pooled from two experiments, each performed in triplicate.

Figure S8. Effects of tryptophan catabolites and AhR inhibitor on intestinal motility, related to Main Figure 7. (A) Experimental model for measuring intestinal motility in response to indole stimulation. (B) EEC Gcamp6f fluorescence (blue line) and changes in intestinal motility (heat map) following indole stimulation. (C) Intestinal μ velocity in response to PBS or indole stimulation. (D) Mean intestinal velocity magnitude 0-50s and 200-250s following indole stimulation. (E) Schematic of experiment design in measuring the effects of indole or IAld in vagal ganglia calcium. WT or EEC ablated *Tg(neurod1:Gcamp6f)*; *Tg(neurod1:TagRFP)* zebrafish that were gavaged with indole or IAld. (F) Quantification of the Gcamp6f to TagRFP fluorescence ratio in the whole vagal sensory ganglia in WT or EEC ablated zebrafish 30 mins following indole gavage. (G) Schematic of experiment design in testing the effects of AhR inhibitors on intestinal *E. tarda* accumulation. To test whether AhR is involved in Trpa1+EEC induced intestinal motility, we applied two well-established AhR inhibitors, CH223191 and folic acid. (H) Representative image of DMSO or AhR inhibitor CH223191 treated zebrafish that were infected with *E. tarda* expressing mCherry (*E. tarda* mCherry). (I) Quantification of *E. tarda* mCherry fluorescence in DMSO, AhR inhibitor CH223191 or Folic acid treated zebrafish intestine. (J) Schematic of experimental design to examine effects of AhR inhibitors on Trpa1+EEC induced intestinal motility. (K) Quantification of mean intestinal velocity magnitude in DMSO, CH223191 or Folic acid treated zebrafish before and post UV activation. Treatment of zebrafish with these AhR inhibitors was insufficient to block *E. tarda* intestinal accumulation. (L) Quantification of mean intestinal velocity magnitude change in DMSO, CH223191 or Folic acid treated zebrafish upon UV-induced Trpa1+EEC activation. Treatment of zebrafish with these AhR inhibitors was insufficient to block Optovin-UV induced intestinal motility change. (M) Schematic of small intestine and colonic regions in 10-week old SPF C57Bl/6 mice that were collected for HPLC-MS analysis. (N) Chemical profiles of Trp-Indole derivatives from colon and small intestine of conventionally-reared mice. Relative amounts of the Trp-metabolites from each mouse was normalized by tissue weight. M1-M3: males. M4-M5: females. Extracted ions were selected for Indole (m/z 117), IAld (m/z 145), and IET, (m/z 161). One-way ANOVA with Tukey's post test was used in F, I, L. ** P<0.01, **** P<0.0001, n.s. not significant.

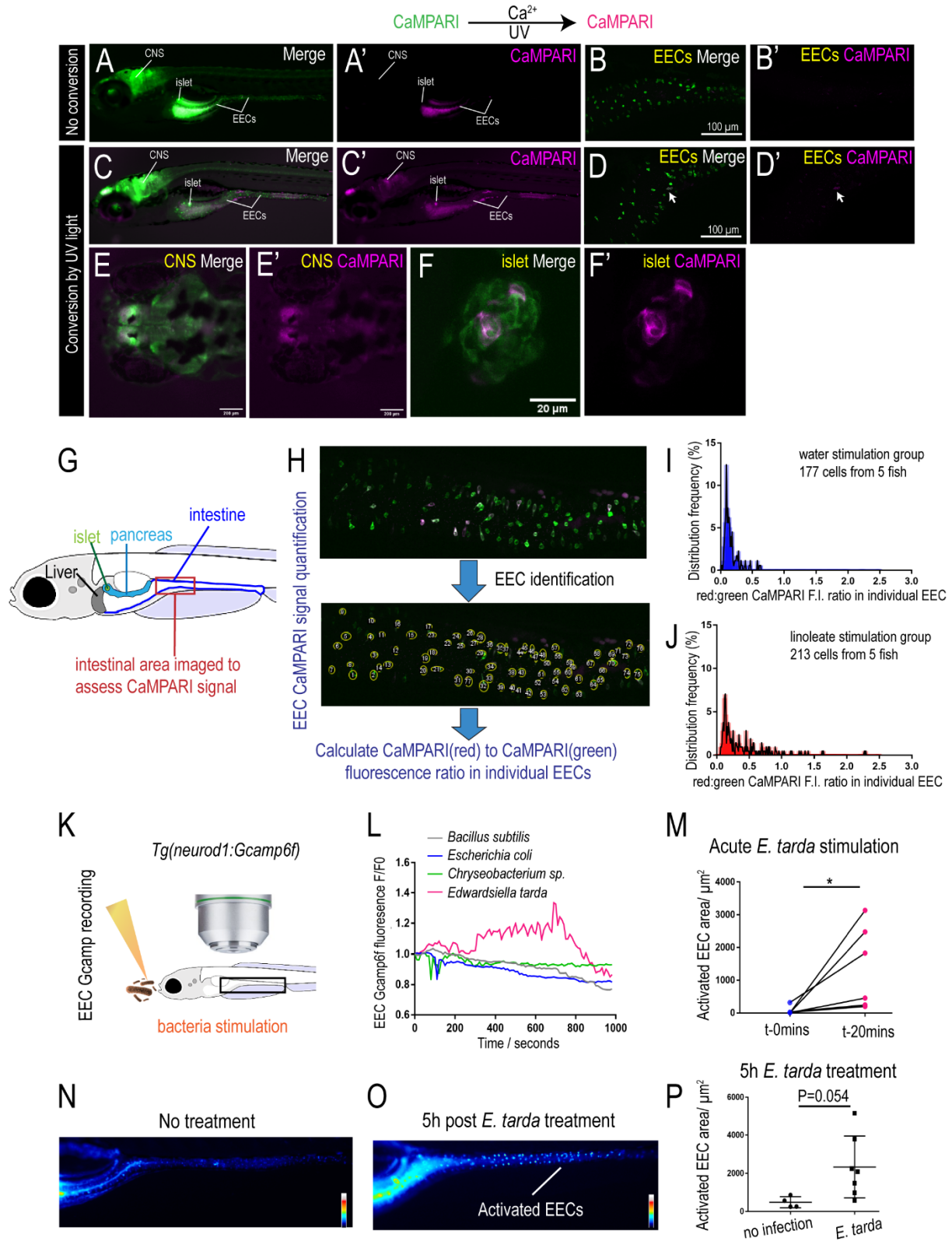


Figure S1. *E. tarda* activates EECs *in vivo*, related to Figure 1.

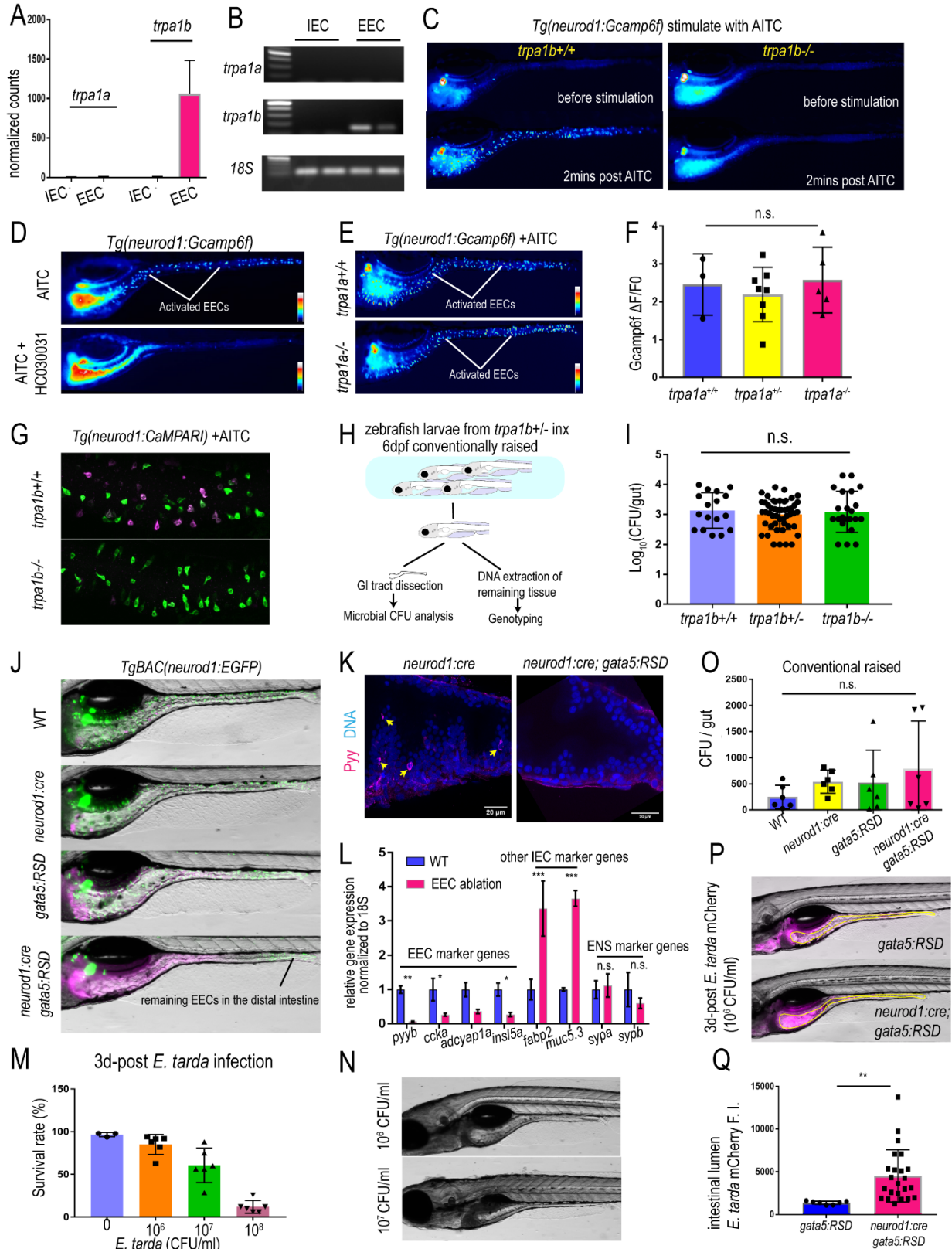


Figure S2. EECs express *trpa1b* and respond to Trpa1 agonist, related to Main Figure 2 and Figure 3.

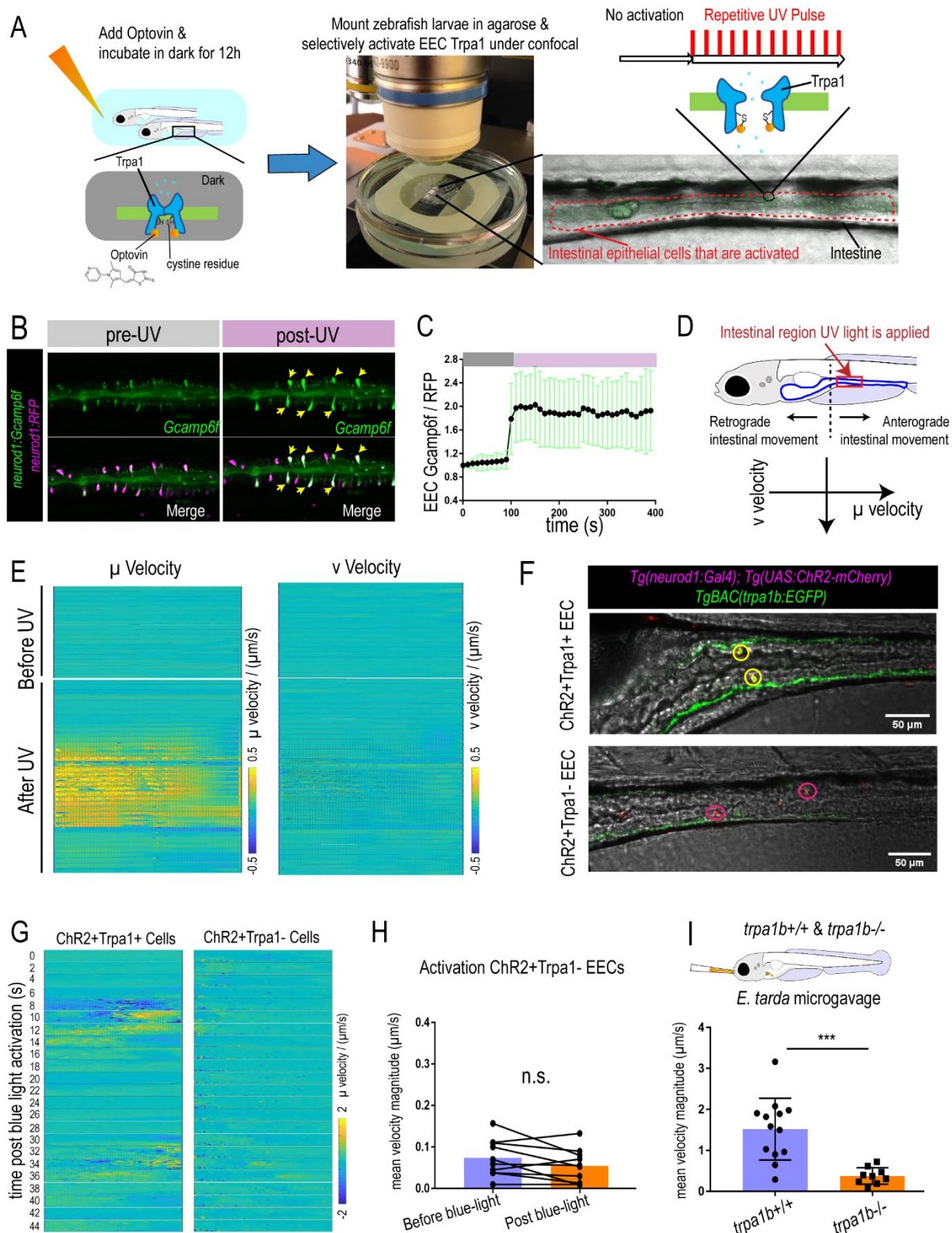


Figure S3. Activation of EEC Trpa1 signaling promotes intestinal motility, related to Main Figure 4.

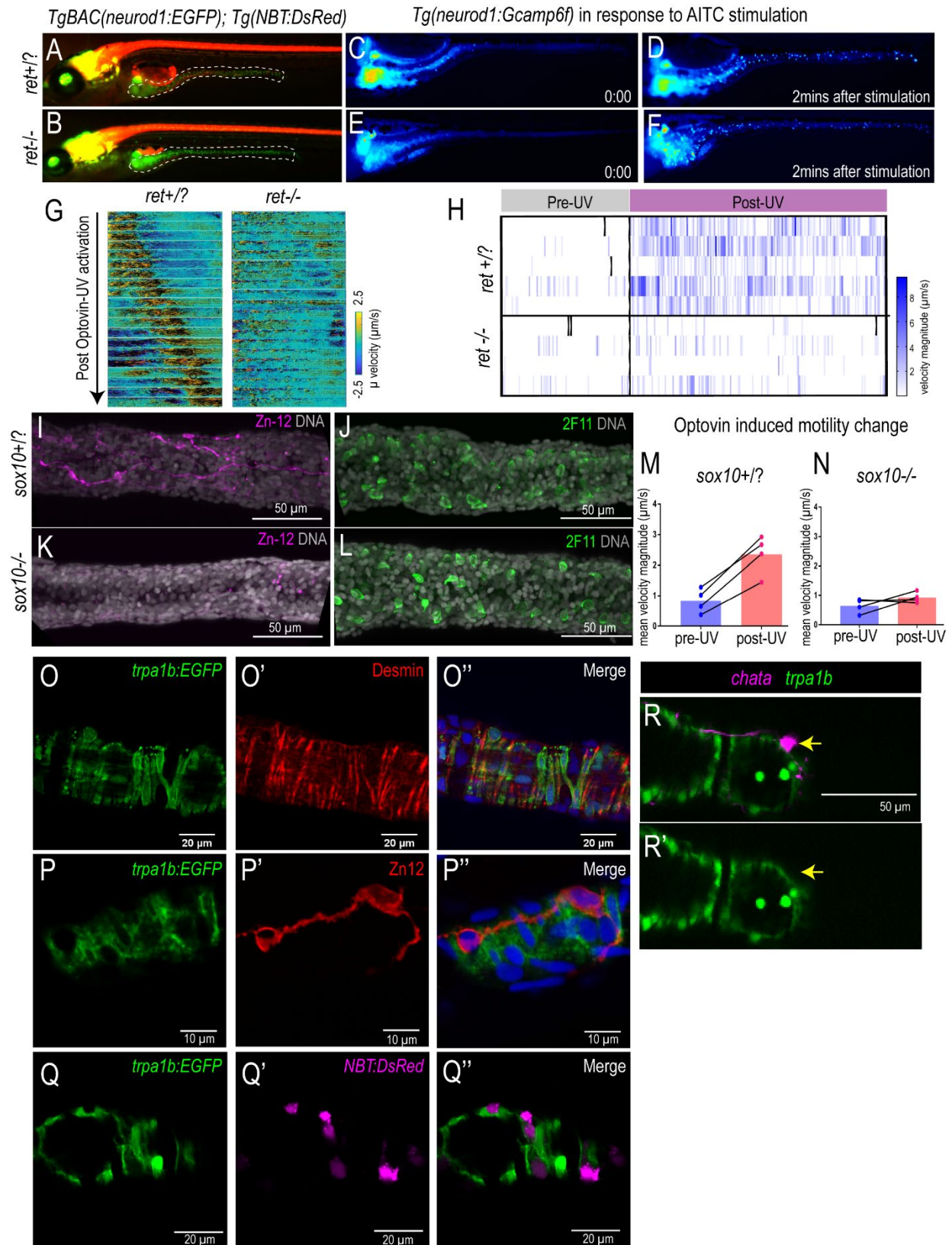


Figure S4. The role of the enteric nervous system in EEC Trpa1-induced intestinal motility, related to Main Figure 5.

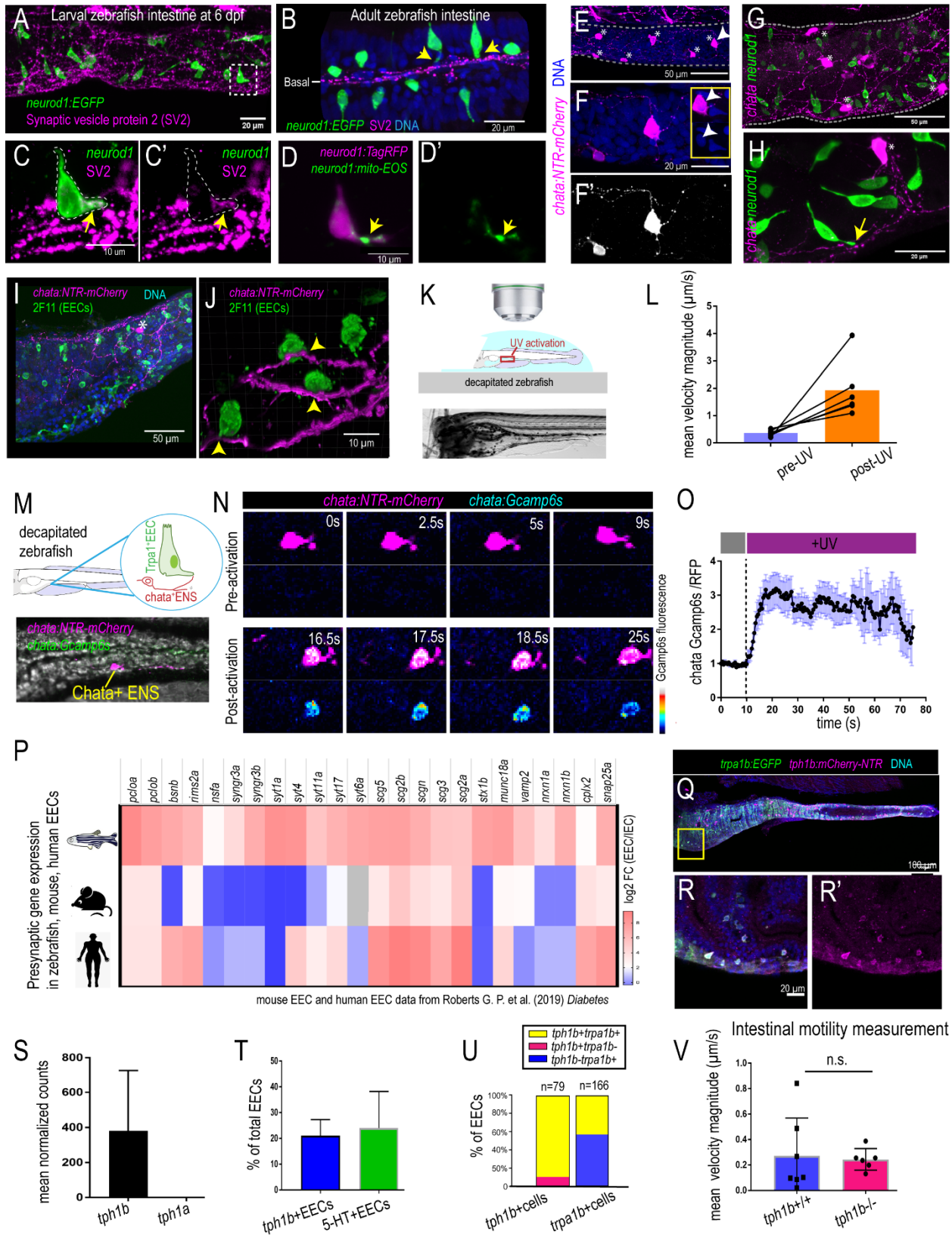


Figure S5. Zebrafish EECs directly communicate with *chata*⁺ ENS, related to Main Figure 5.

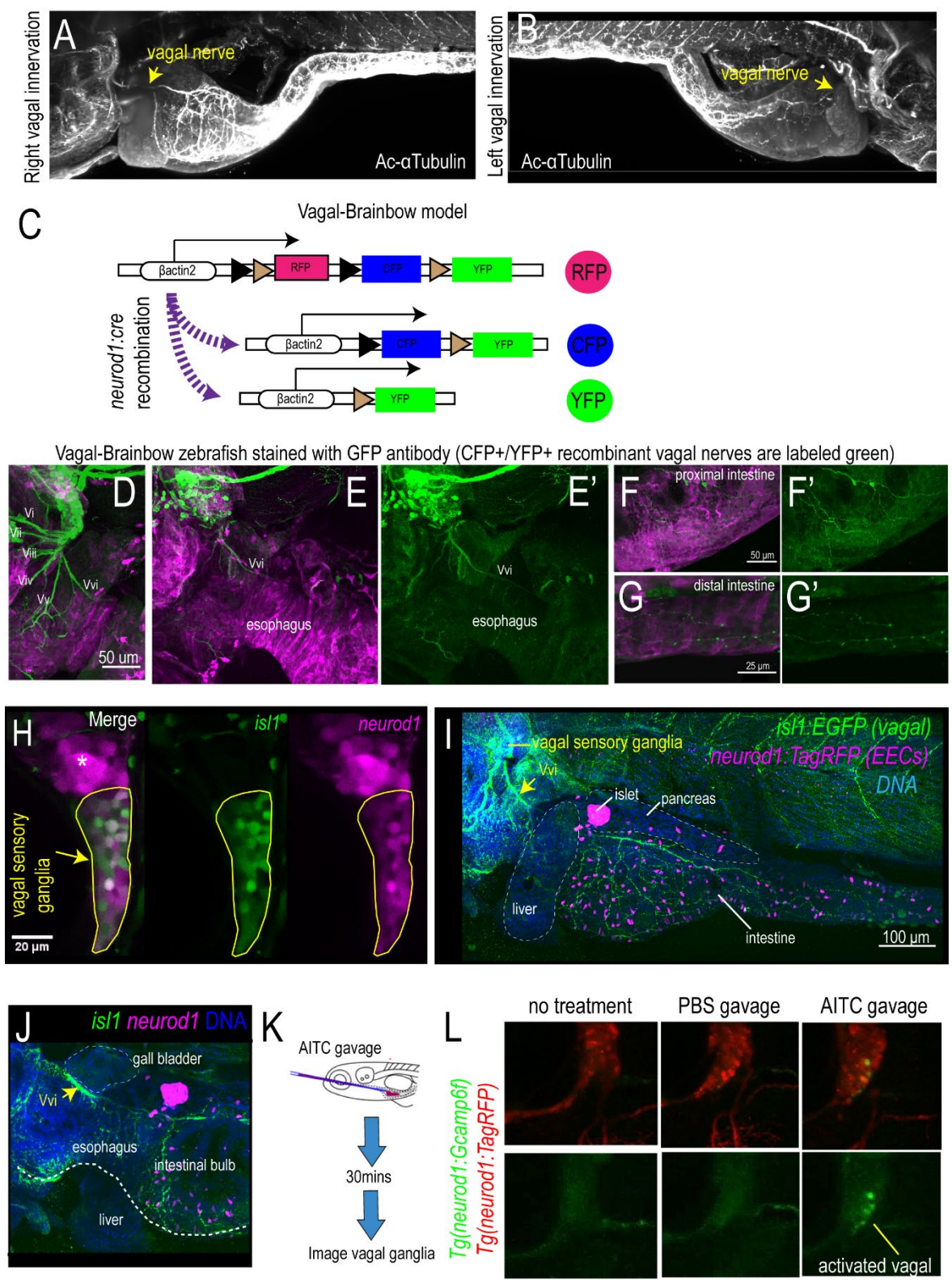


Figure S6. Zebrafish vagal sensory nerves innervate the intestine, related to Main Figure 6.

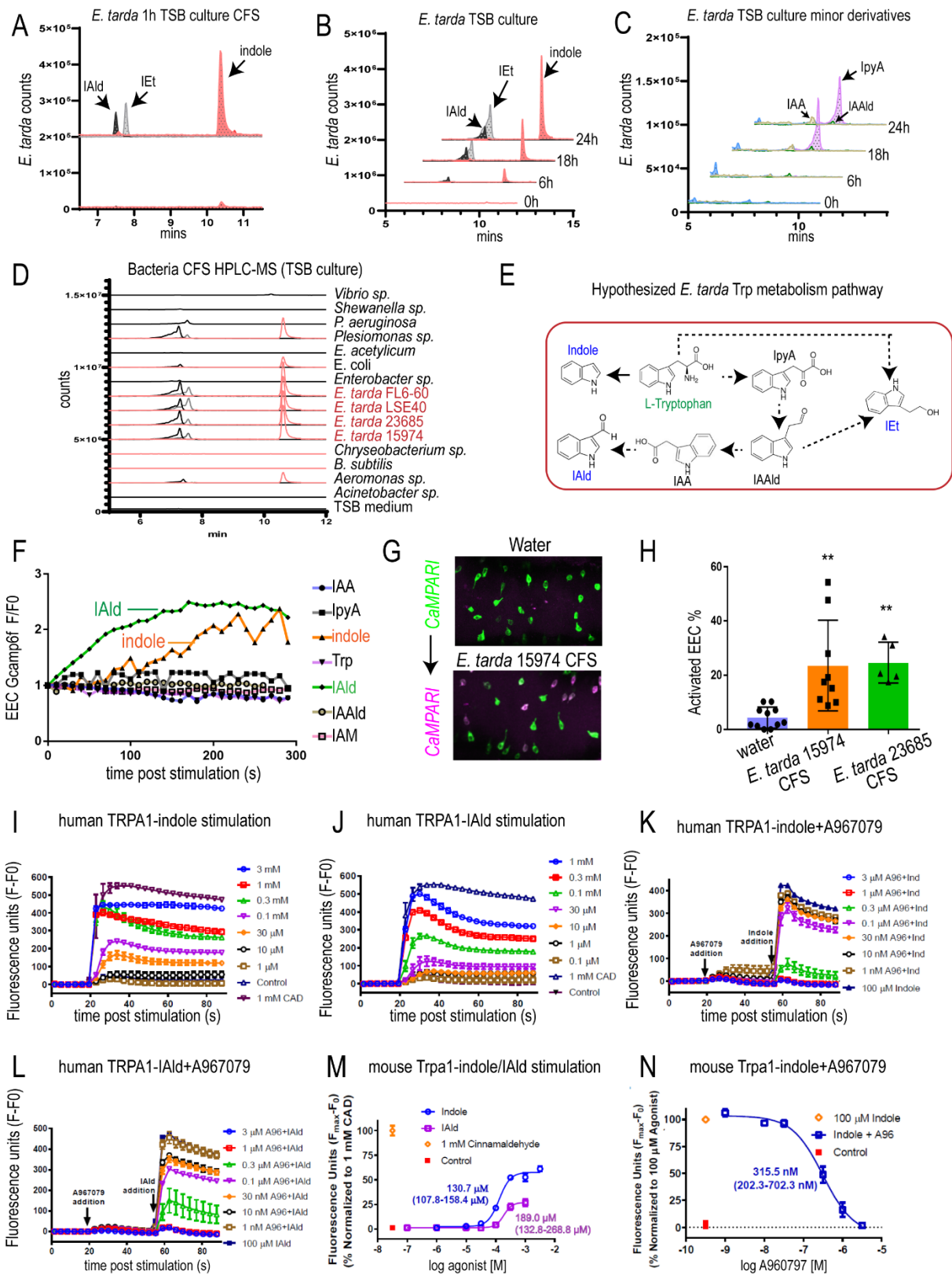


Figure S7. *E. tarda* secretes tryptophan catabolites indole and IAld that activate Trpa1, related to Main Figure 7.

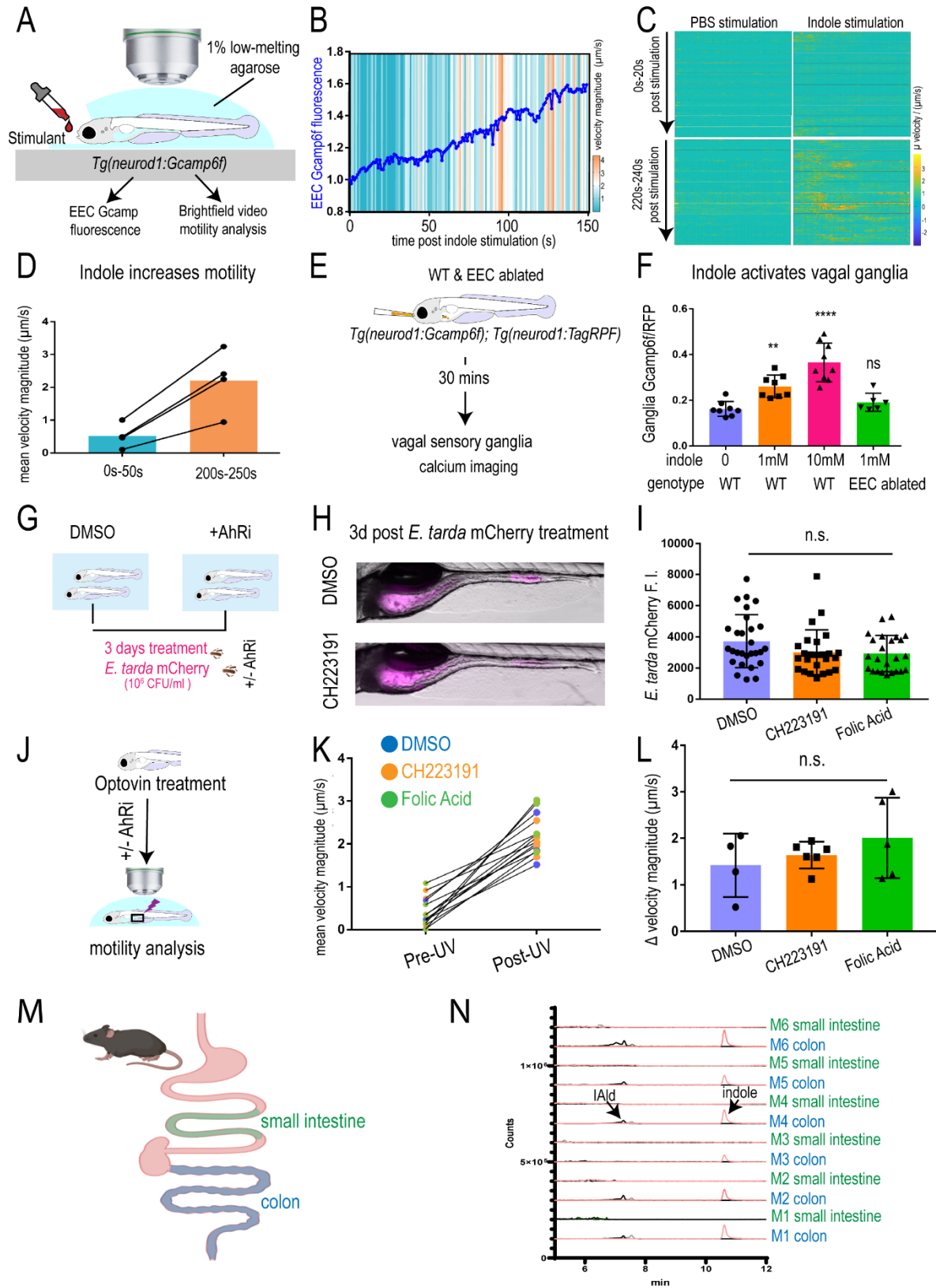


Figure S8. Effects of tryptophan catabolites and AhR inhibitor on intestinal motility, related to Main Figure 7.